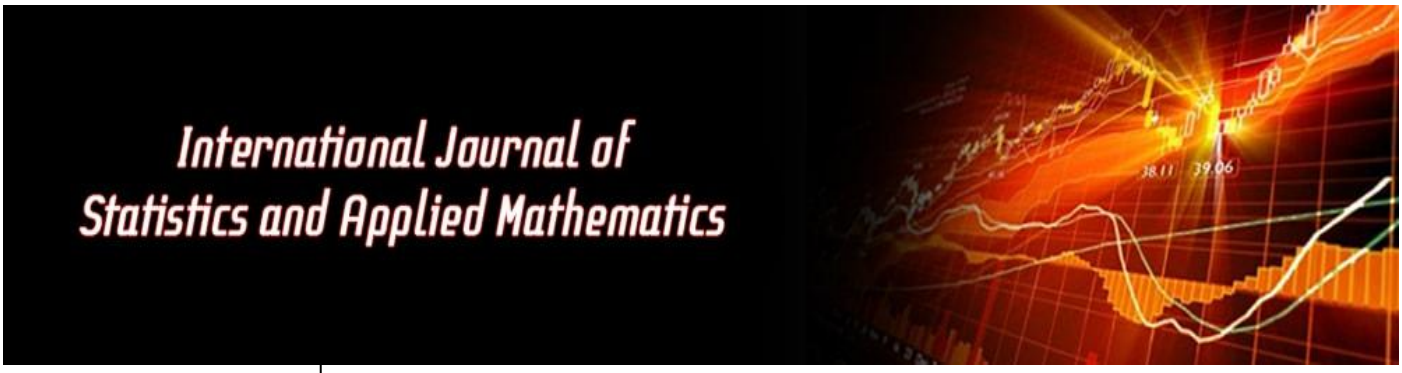

ISSN: 2456-1452
Maths 2018; 3(4): 16-26

www.mathsjournal.com
Received: 03-05-2018
Accepted: 04-06-2018

S Sampathraj
Research Scholar, Department of Mathematics, Pachiyappa's College, Chennai, Tamil Nadu, India

K Thangavelu
Principal, C. Kandaswami Naidu College, Chennai, Tamil Nadu, India

V Sudha
Assistant Professor,Department of Mathematics, Sri Kanyaka Parameswari Arts & Science College for Women, Chennai, Tamil Nadu, India

Correspondence
S Sampathraj
Research Scholar, Department of Mathematics, Pachiyappa's College, Chennai, Tamil Nadu, India

Effects of slip-velocity and viscosity variation in squeeze film lubrication of triangular plates

S Sampathraj, K Thangavelu and V Sudha

Abstract
An effort has been made to analyse the squeeze film effects of triangular plates. A generalized form of Reynolds equation governing the flow for two symmetrical surfaces is studied. The velocity profile governing the flow is derived and the expressions for load carrying capacity and squeeze time are obtained. Theoretical analysis of slip velocity and the viscosity variations of triangular plates have also been discussed in this paper.

Keywords: Reynolds equation, squeeze film, squeeze time and squeeze pressure

1. Introduction
Squeeze film lubrication has several practical applications in our day today life. The performance of hydraulic machines are enhanced in the presence of squeeze film lubrication. Squeeze film phenomenon is found when two relatively moving surfaces approach each other with a normal velocity. The viscous lubricant between the plates offers resistance to extrusion and builds up pressure that helps to support the load. Dowson [1] developed a generalised form of Reynolds equation which permits the variation of relevant quantities across, as well as along the lubricant film. Squeeze film characteristics of couple stress fluid between porous triangular plates is analysed in [2]. The micro additives present in the lubricant enhances the squeeze film characteristics. Vadher [3] analysed hydro magnetic squeeze film between conducting porous transversely rough triangular plates. The results shows that the magnetization parameter and the conductivity increase the load carrying capacity while, the load carrying capacity decreases due to porosity and standard deviation. Sundarammal Kesavan and Manimegalai [4] investigated the surface roughness effects on the squeeze film between two parallel porous elliptic plates. The surface roughness and the couple stress present in the lubricant results in high lubricant viscosity. Hamid Khan [7] studied the effects of squeeze flow between two large parallel plates by transforming the basic governing equations of the first grade fluid to an ordinary nonlinear differential equation using the stream functions and a transformation.
Rao [9] analysed the effects of velocity-slip and viscosity variation for squeeze film lubrication of two circular plates. The load capacity and squeeze time decreases due to slip. Fathima [11] studied the combined effect of couple stress and magnetic effect on the squeeze film lubrication between porous plates of different geometry. The effect of the porous facing on couplestress squeeze film lubrication in the presence of applied magnetic field enhances pressure, load carrying capacity and squeeze film time. The results are compared to corresponding non-magnetic and Newtonian case. Umar Khan [12] applied the variation of parameters method can successfully be applied to solve the equations governing unsteady squeezing flows between parallel plates. Santhana Krishnan Narayanan and Sundarammal Kesavan [13], analysed the magneto-hydrodynamics non-newtonian squeeze film characteristics of porous circular plates. We have analysed the effects of viscosity variation in squeeze film lubrication of circular stepped plates in [14]. In the present paper, an attempt has been made to study the effects of slip velocity and viscosity variation in squeeze film lubrication of triangular plates.

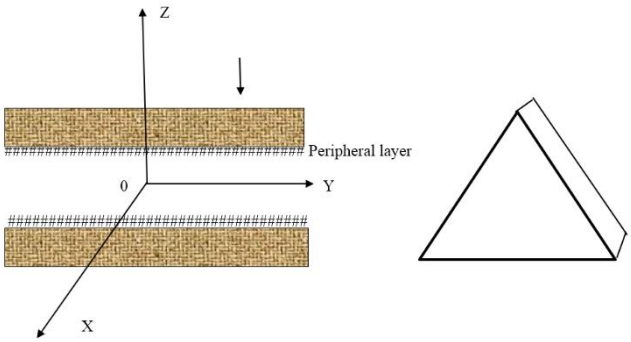

Fig 1: Squeeze film between two triangular Plates

2. Nomenclature

h	Total film thickness
h_f	Final film thickness
p	Pressure
p^*	Expected value of the pressure
v	Squeeze velocity
α	Variance
w	Load capacity
μ	Viscosity of the purely hydrodynamic zone
a	The length of the side of the equilateral triangle
h	Film thickness
h^*	Dimensionless film thickness $\left(= h/h_0 \right)$
h_0	Minimum film thickness (when time t = 0)
h_1	Film thickness after time Δt
x, y, z	Cartesian coordinates
t	Squeeze time
T^*	Non-dimensional time
W	Load carrying capacity
w^*	Non-dimensional load carrying capacity
η	Material constant
k	Ratio of the viscosities

$$x^* = \frac{x_1}{a}$$

$$y^* = \frac{y_1}{a}$$

$$h^* = \frac{h}{h_0}$$

3. Analysis

The Navier-Stokes equation for the laminar flow between two symmetric plates as obtained by Dowson [1] is,

$$\frac{\partial p}{\partial x} - \frac{\partial}{\partial z}\left[\eta \frac{\partial u}{\partial z}\right] = 0 \quad (1)$$

$$\frac{\partial p}{\partial x} - \frac{\partial}{\partial z}\left[\eta \frac{\partial v}{\partial z}\right] = 0 \quad (2)$$

$$\frac{\partial \rho}{\partial t}+\frac{\partial(\rho u)}{\partial x}+\frac{\partial(\rho v)}{\partial y}+\frac{\partial(\rho w)}{\partial z}=0 \tag{3}$$

Where p= p(x, y) is the pressure in the film and η is the viscosity. The boundary conditions considering slip at the surfaces.

$$u=(u)_1=(\lambda)_1\left[\frac{\partial u}{\partial z}\right]_1+U_1$$
$$v=(v)_1=(\delta)_1\left[\frac{\partial v}{\partial z}\right]_1+V_1$$
$$at\ Z=H_1$$

$$u=(u)_2=-(\lambda)_2\left[\frac{\partial u}{\partial z}\right]_2+U_2$$
$$v=(v)_2=-(\delta)_2\left[\frac{\partial v}{\partial z}\right]_2+V_2 \tag{4}$$
$$at\ Z=H_2$$

Where the suffixes 1 and 2 represent the values at $z=H_1$ and $z=H_2$, respectively. Here λ and δ depend on viscosity and the coefficient is sliding friction.
From equation (1), (2) and (4) we obtain,

$$u-\left[\alpha_1 H_1+\int_{H_1}^{z}\frac{z\,dz}{\eta}\right]\frac{\partial p}{\partial x}=U_1+\left[\alpha_1+\int_{H_1}^{z}\frac{dz}{\eta}\right]\left[\frac{U_2-U_1}{F_0}-\frac{F_1}{F_0}\frac{\partial p}{\partial x}\right]$$

$$v-\left[\beta_1 H_1+\int_{H_1}^{z}\frac{z\,dz}{\eta}\right]\frac{\partial p}{\partial y}=V_1+\left[\beta_1+\int_{H_1}^{z}\frac{dz}{\eta}\right]\left[\frac{V_2-V_1}{F^1{}_0}-\frac{F^1{}_1}{F^1{}_0}\frac{\partial p}{\partial y}\right] \tag{5}$$

Where $F_0=\alpha_1+\alpha_2+\int_{H_1}^{Z}\frac{dz}{\eta}$, $F^1{}_0=\beta_1+\beta_2+\int_{H_1}^{z}\frac{z\,dz}{\eta}$,

$F_1=\alpha_1 H_1+\alpha_2 H_2+\int_{H_1}^{H_2}\frac{z\,dz}{\eta}$, $F_1^1=\beta_1 H_1+\beta_2 H_2+\int_{H_1}^{z}\frac{z\,dz}{\eta}$

$$\alpha_1=\frac{(\lambda)_1}{(\eta)_1},\ \alpha_2=\frac{(\lambda)_2}{(\eta)_2},\ \beta_1=\frac{(\delta)_1}{(\eta)_1},\ \beta_2=\frac{(\delta)_2}{(\lambda)_2} \tag{6}$$

From equation (3)

$$\int_{H_1}^{H_2}\frac{\partial \rho}{\partial t}dz+\int_{H_1}^{H_2}\frac{\partial(\rho u)}{\partial x}dz+\int_{H_1}^{H_2}\frac{\partial(\rho v)}{\partial y}dz+(\rho w)_{H_1}^{H_2}=0 \tag{7}$$

$$\frac{\partial}{\partial x}\left\{(F_2+G_1)\frac{\partial p}{\partial x}\right\}+\frac{\partial}{\partial y}\left\{\left(F_2^1+G_1^1\right)\frac{\partial p}{\partial y}\right\}+H_1\left\{\frac{\partial}{\partial x}(\rho u)_1+\frac{\partial}{\partial y}(\rho v)_1\right\}$$
$$=H_2\left\{\frac{\partial}{\partial x}(\rho u)_2+\frac{\partial}{\partial y}(\rho v)_2\right\}+\int_{H_1}^{H_2}\frac{\partial \rho}{\partial y}dz+(\rho w)_{H_1}^{H_2} \tag{8}$$

Where $F_2=\int_{H_1}^{H_2}\frac{\rho z}{\eta}\left[z-\frac{F_1}{F_0}\right]dz$, $F_2^1=\int_{H_1}^{H_2}\frac{\rho z}{\eta}\left[z-\frac{F_1^1}{F_0^1}\right]dz$, $F_3=\int_{H_1}^{H_2}\frac{\rho z}{\eta}dz$,

$$G_1=\int_{H_1}^{H_2}\left[z\frac{\partial\rho}{\partial z}\left\{\alpha_1 H_1+\int_{H_1}^{z}\frac{z\,dz}{\eta}-\frac{F_1}{F_0}\left[\alpha_1+\int_{H_1}^{z}\frac{dz}{\eta}\right]\right\}\right]dz,$$

$$G_1{}^1=\int_{H_1}^{H_2}\left[z\frac{\partial\rho}{\partial z}\left\{\beta_1 H_1+\int_{H_1}^{z}\frac{z\,dz}{\eta}-\frac{F_1}{F_0}\left[\beta_1+\int_{H_1}^{z}\frac{dz}{\eta}\right]\right\}\right]dz$$

$$G_2=\int_{H_1}^{H_2}\left\{z\frac{\partial\rho}{\partial z}\left[\alpha_1+\int_{H_1}^{z}\frac{dz}{\eta}\right]\right\}dz$$

$$G_2^1=\int_{H_1}^{H_2}\left\{z\frac{\partial\rho}{\partial z}\left[\beta_1+\int_{H_1}^{z}\frac{dz}{\eta}\right]\right\}dz, G_3=\int_{H_1}^{H_3}z\frac{\partial\rho}{\partial z}dz \tag{9}$$

Assuming slip conditions at the bearing surfaces,

$$(\lambda)_1=(\lambda)_2=(\delta)_1=(\delta)_2=0$$

$$\alpha_1=\alpha_2=\beta_1=\beta_2=0$$

Using the concept of multiple layer lubrication,

$$\rho=\rho_1(x,y),\eta=\eta_1(x,y) \qquad H_1\le z\le H_1+h_1$$

$$\rho=\rho_2(x,y),\eta=\eta_2(x,y) \qquad H_1+h_1\le z\le H_1+h_1+h_2$$

$$\rho=\rho_3(x,y),\eta=\eta_3(x,y) \qquad H_1+h_1+h_2\le z\le H_1+h_1+h_2+h_3 \tag{10}$$

Assuming, $U_1= U$ $U_2=V_1=V_2=0$

$$\alpha_1=\beta_1 \qquad \alpha_2=\beta_2$$

$$\frac{\partial\rho_i}{\partial z}=0 \qquad \text{i=1, 2, 3} \tag{11}$$

From equation (8),

$$\frac{\partial}{\partial x}\left[F_2\frac{\partial p}{\partial x}\right]+\frac{\partial}{\partial y}\left[F_2\frac{\partial p}{\partial y}\right]=H_2\left\{\frac{\partial}{\partial x}(\rho u)_2+\frac{\partial}{\partial y}(\rho v)_2\right\}-H_1\left\{\frac{\partial}{\partial x}(\rho u)_1+\frac{\partial}{\partial y}(\rho v)_1\right\}$$

$$+U\frac{\partial}{\partial x}\left[\frac{F_3}{F_0}\right]+[\rho w]_{H_1}^{H_2} \tag{12}$$

Where $F_0=\alpha_1+\alpha_2+\frac{h_1}{\eta_1}+\frac{h_2}{\eta_2}+\frac{h_3}{\eta_3}$

$$F_1=\alpha_1 H_1+\alpha_2 H_2+\frac{h_1(2H_1h_1)}{2\eta_1}+\frac{h_2(2H_1+2h_1+h_2)}{2\eta_2}+\frac{h_3(2H_1+2h_1+2h_2+h_3)}{2\eta_3}$$

$$F_2 = \frac{\rho_1}{3\eta_1}\left\{(H_1 + h_1)^3 - H_1^3\right\} + \frac{\rho_1}{3\eta_2}\left\{(H_1 + h_1 + h_2)^3 - (H_1 + h_1)^3\right\} + \frac{\rho_3}{3\eta_3}\left\{H_2^3 - (H_1 + h_1 + h_2)^3\right\} - \frac{F_1 F_3}{F_0}$$

$$F_3 = \frac{\rho_1 h_1 (2H_1 h_1)}{2\eta_1} + \frac{\rho_2 h_2 (2H_1 + 2h_1 + h_2)}{2\eta_2} + \frac{\rho_3 h_3 (2H_1 + 2h_1 + 2h_2 + h_3)}{2\eta_3}$$

$$(\rho u)_1 = \rho_1 \alpha_1 \left[H_1 - \frac{F_1}{F_0} \right] \frac{\partial P}{\partial x} + \rho_1 U \left[1 - \frac{\alpha_1}{F_0} \right]$$

$$(\rho u)_2 + \rho_3 \alpha_2 \left[H_2 - \frac{F_1}{F_0} \right] \frac{\partial P}{\partial x} = \rho_3 U \frac{\alpha_2}{F_0}$$

$$(\rho v)_1 = \rho_1 \alpha_1 \left[H_1 - \frac{F_1}{F_0} \right] \frac{\partial P}{\partial y}$$

$$(\rho v)_2 + \rho_3 \alpha_2 \left[H_2 - \frac{F_1}{F_0} \right] \frac{\partial P}{\partial y} = 0 \tag{13}$$

$$[\rho w]_{H_1}^{H_2} + (\rho u)_1 \frac{\partial H_1}{\partial x} + (\rho v)_1 \frac{\partial H_1}{\partial y} + V_s = (\rho u)_2 \frac{\partial H_2}{\partial x} + (\rho v)_2 \frac{\partial H_2}{\partial y}$$

Where V_s is the resultant velocity towards the film. Considering three symmetrical incompressible layers between two solid boundaries we have,

$\eta_1 = \eta_2$ and $\rho_1 = \rho_2 = \rho_3$

Taking $H_1=0$, $H_2 = (h + a) = h, h_1 = h_3 = a/2, h_2 = (h - a)$ and

$$\alpha_1 = \alpha_2 = \beta_1 = \beta_2 = 1/\beta \tag{14}$$

Hence,

$$\frac{\partial}{\partial x}\left[F_4 \frac{\partial p}{\partial x} \right] + \frac{\partial}{\partial y}\left[F_4 \frac{\partial p}{\partial y} \right] = U \frac{\partial}{\partial x}(h) - V \tag{15}$$

Where $F_4 = \frac{(h-a)^3}{12\eta_2} + \frac{a^3 + 3a^2(h-a) + 3a(h-a)^2}{12\eta_1} + \frac{h^2}{2\beta}$, $\beta = \frac{\eta_1}{\lambda}$ is the slip parameter.

In the case of squeeze film lubrication of triangular plates we have,

$$\frac{\partial^2 p}{\partial x^2} + \frac{\partial^2 p}{\partial y^2} = \frac{12\mu\, dh/dt}{F_4} \tag{16}$$

The boundary conditions for the pressure field are,

$$p(x_1, y_1) = 0 \tag{17}$$

Where $(x_1 - a)\left(x_1 - \sqrt{3}y_1 + 2a\right)\left(x_1 + \sqrt{3}y_1 + 2a\right) = 0$

Hence the pressure is obtained as,

$$p = -\frac{12\mu\, dh/dt}{F_4}\frac{a^2}{3}\left(1-\frac{3}{4a^2}x_1^2-\frac{3}{4a^2}y_1^2-\frac{1}{4a^3}x_1^3+\frac{3}{4a^3}x_1y_1^2\right) \tag{18}$$

The dimensionless pressure of the bearing is,

$$p^* = -\frac{ph_0^3}{\mu\,(dh/dt)3\sqrt{3}a^2} = \frac{4}{\sqrt{3}F_4}\left(1-\frac{x^*}{a}\right)\left(1+\frac{\sqrt{3}y^*}{2a}+\frac{x^*}{2a}\right)\left(1-\frac{\sqrt{3}y^*}{2a}+\frac{x^*}{2a}\right) \tag{19}$$

Integrating the pressure over the area of the plate the load carrying capacity of the bearing is,

$$W = \int_{-2a}^{a}\int_{-\left(\frac{2a+x_1}{\sqrt{3}}\right)}^{\left(\frac{2a+x_1}{\sqrt{3}}\right)} p\,dy_1\,dx_1 \tag{20}$$

$$W = -\frac{12\mu\, dh/dt}{F_4}\left[\frac{27\sqrt{3}a^4}{60}\right]$$ The load carrying capacity of bearing in non-dimensional form is,

$$W^* = -\frac{Wh_0^3}{27\mu\,(dh/dt)a^4} = \frac{\sqrt{3}}{5F_4} \tag{21}$$

The time-height relation is observed to be

$$t = -\frac{27\sqrt{3}a^4}{5W}\int_{h_0}^{h_1}\frac{dh}{F_4} \tag{22}$$

Time-height relation in dimensionless form is,

$$T^* = \int_1^{t_1/t_0}\frac{Wh_0^2\,dt}{27\mu a^4} = -\frac{\sqrt{3}}{5}\int_1^{h_1^*}\frac{dh^*}{F_4} \tag{23}$$

4. Discussion and Results

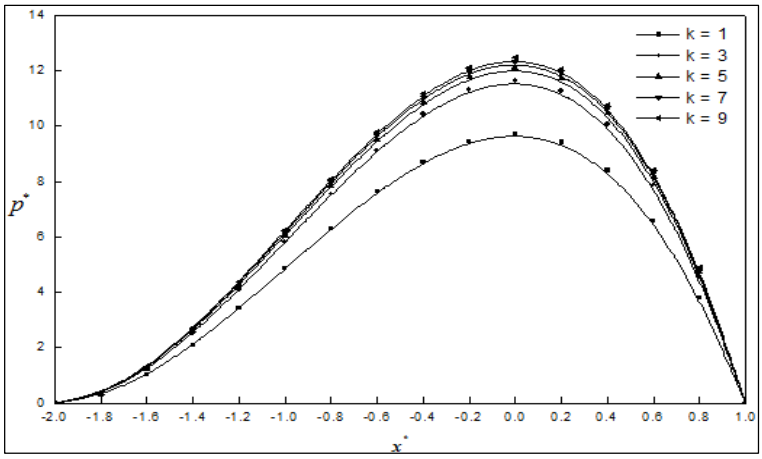

Fig 2: Variation of p^* with x^* for different values of k with $h^* = 0.6, a = 0.06, \beta = 100, y = 0.$

Figure 2, indicates variation of p^* with x^* for $k = 1, k = 3,\ k = 5, k = 7$ and $k = 9$. We observe that for any value of x^* the dimensionless pressure p^* increases for an increase in k.

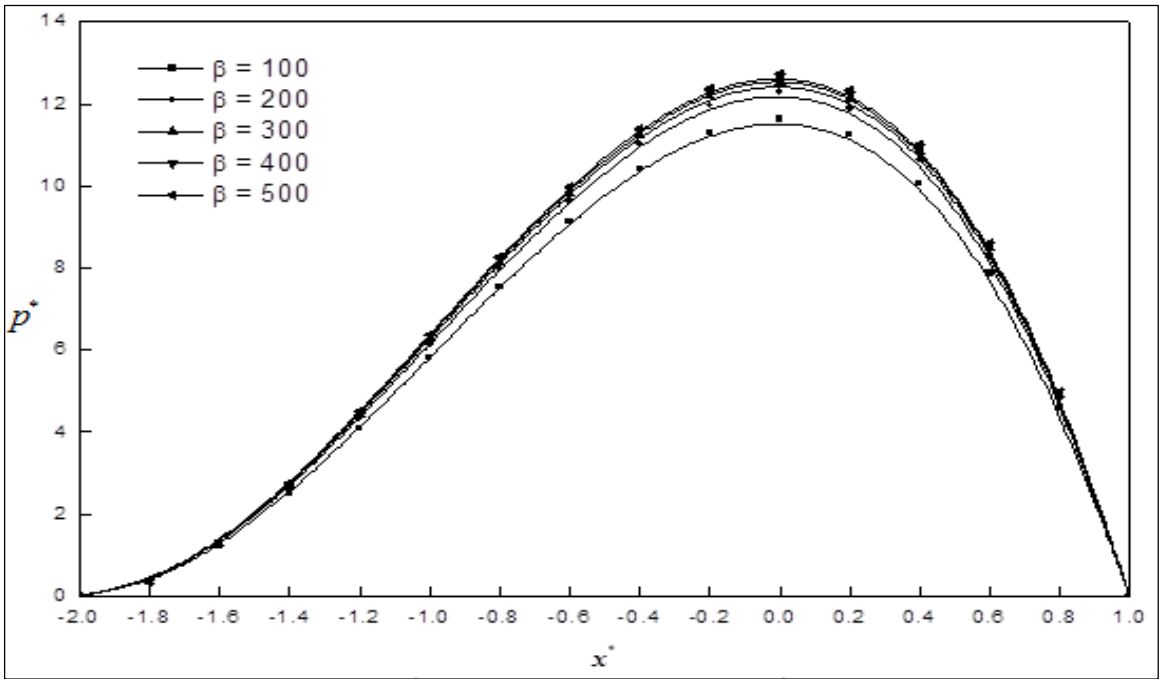

Fig 3: Variation of p^* with x^* for different values of β with $h^* = 0.6, a = 0.06, k = 3, y = 0.$

Figure 3, indicates variation of p^* with x^* for $\beta = 100, \beta = 200, \beta = 300, \beta = 400$ and $\beta = 500$. We observe that for any value of x^* dimensionless pressure p^* increases for an increase in β.

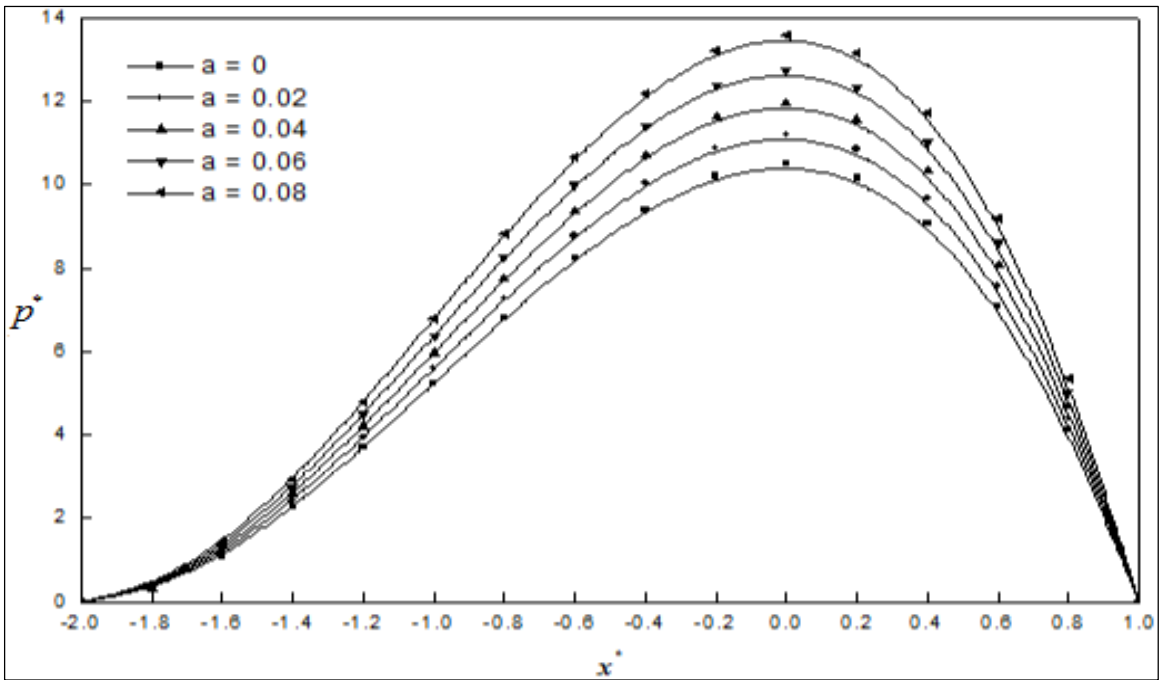

Fig 4: Variation of p^* with x^* for different values of a with $h^* = 0.6, k = 3, \beta = 100, y = 0.$

Figure 4, indicates variation of p^* with x^* for $a = 0, a = 0.02, a = 0.04, a = 0.06$ and $a = 0.08$. We observe that for any value of x^* dimensionless pressure p^* increases for an increase in a.

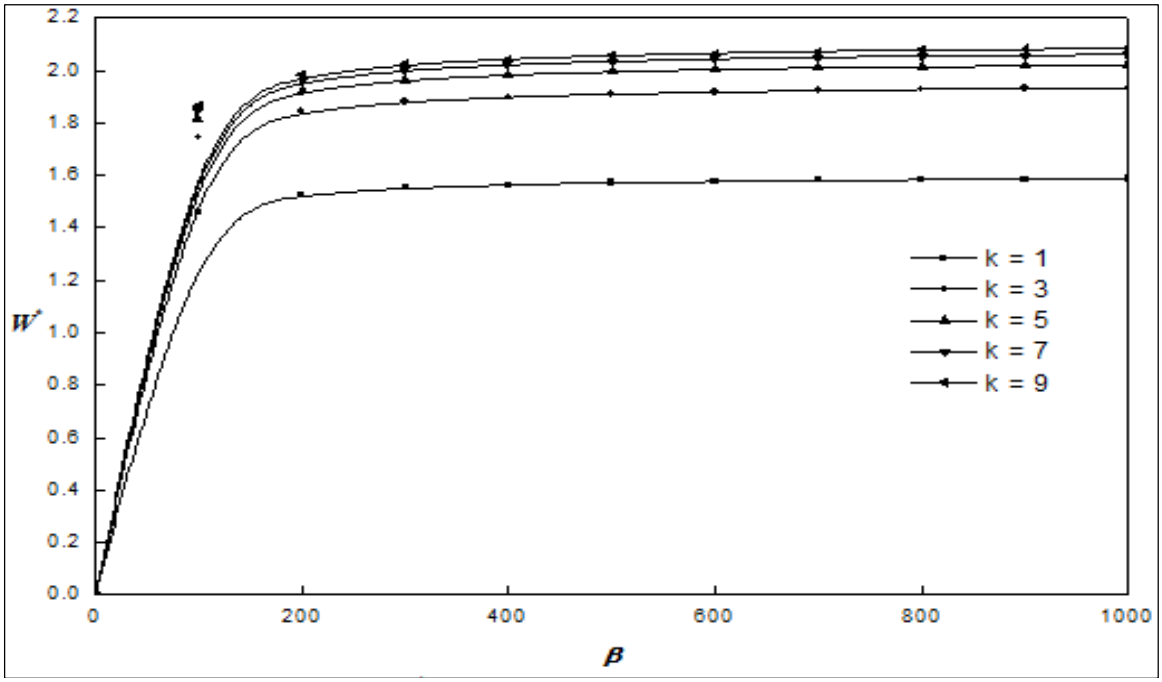

Fig 5: Variation of W^* with β for different values of k with $h^* = 0.6,\ a = 0.06$.

Figure 5, indicates variation of W^* with β for $k = 1, k = 3,\ k = 5, k = 7$ and $k = 9$. We observe that for any value of β dimensionless load carrying capacity W^* increases for an increase in k.

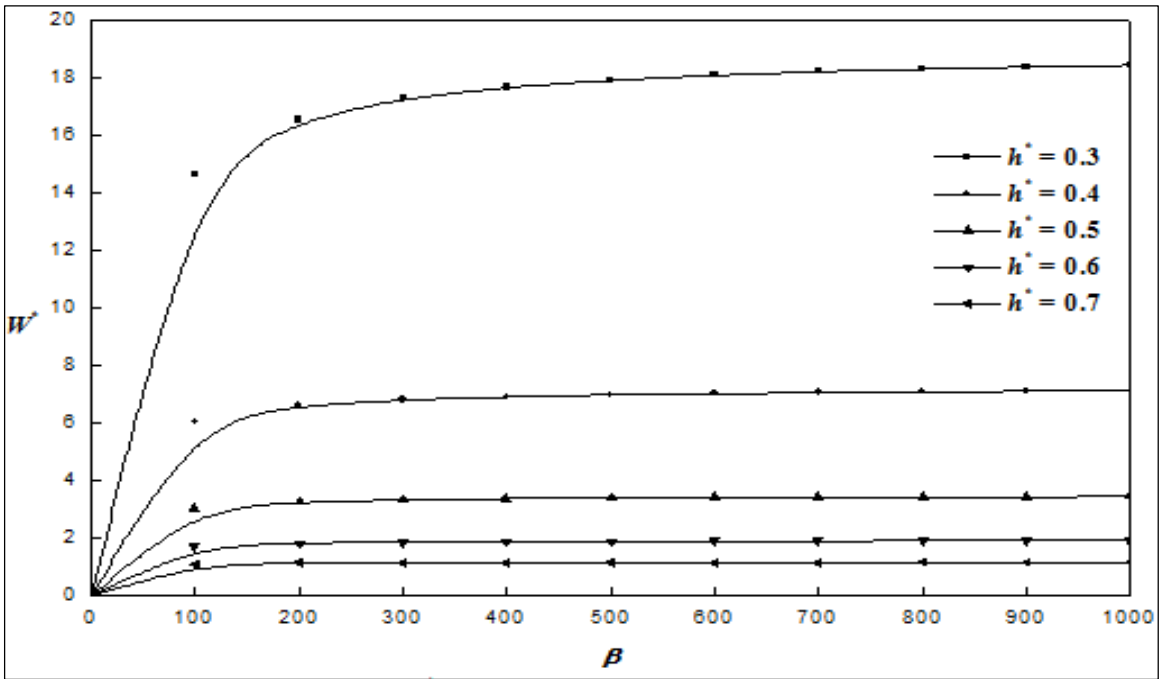

Fig 6: Variation of W^* with β for different values of h^* with $k = 3, a = 0.06$.

Figure 6, indicates variation of W^* with β for $h^* = 0.3,\ h^* = 0.4,\ h^* = 0.5,\ h^* = 0.6$ and $h^* = 0.7$. We observe that for any value of β dimensionless load carrying capacity W^* increases for an increase in h^*.

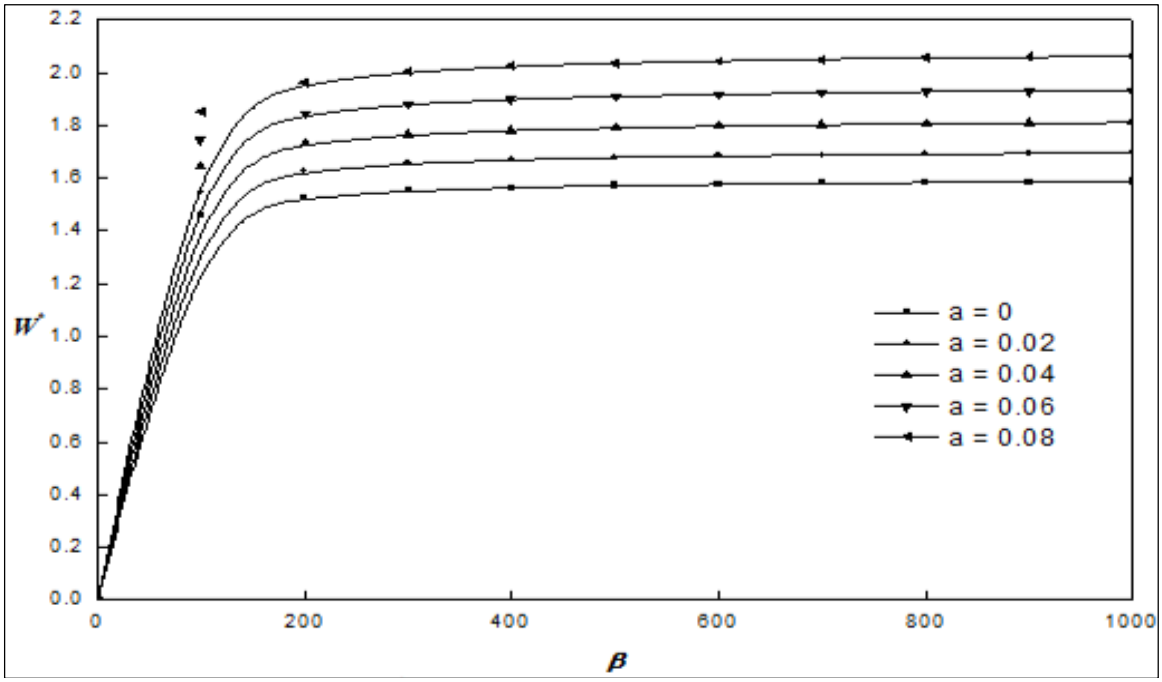

Fig 7: Variation of W^* with β for different values of h^* with $k = 3, a = 0.06$.

Figure 7, indicates variation of W^* with β for $a = 0$, $a = 0.02$, $a = 0.04$, $a = 0.06$ and $a = 0.08$. We observe that for any value of β dimensionless load carrying capacity W^* increases for an increase in a.

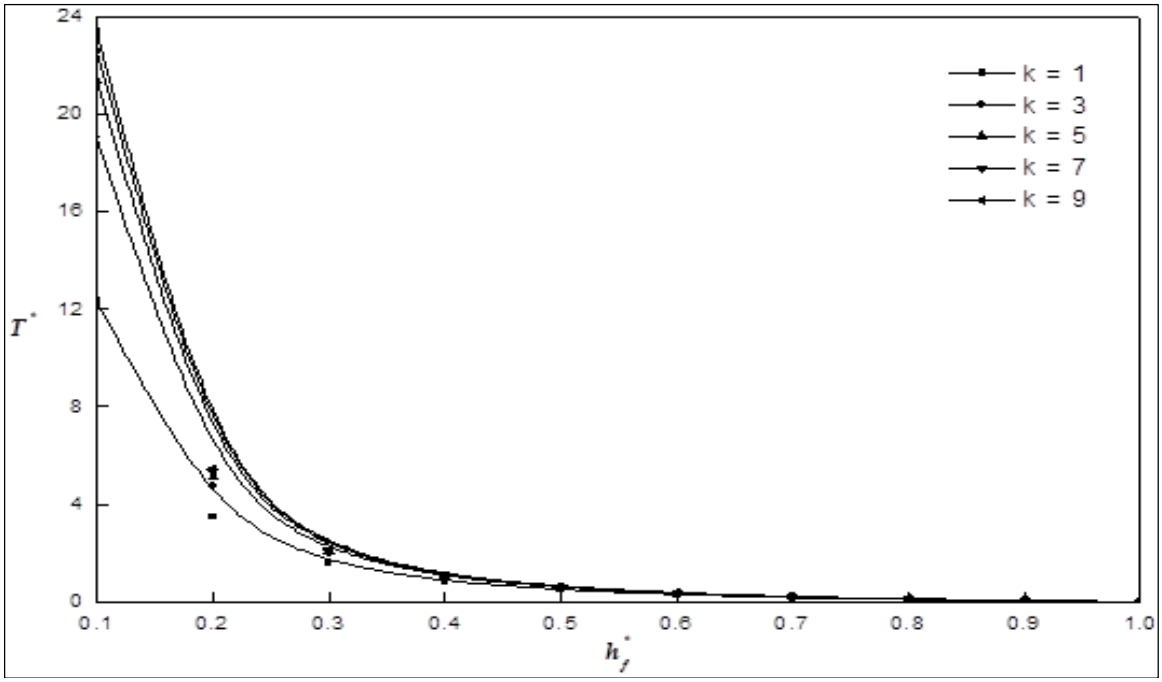

Fig 8: Variation of T^* with h_f^* for different values of k with $\beta = 100, a = 0.06$.

Figure 8, indicates variation of T^* with h_f^* for $k = 1$, $k = 3$, $k = 5$, $k = 7$ and $k = 9$. We observe that for any value of h_f^* dimensionless time T^* decreases for an increase in k.

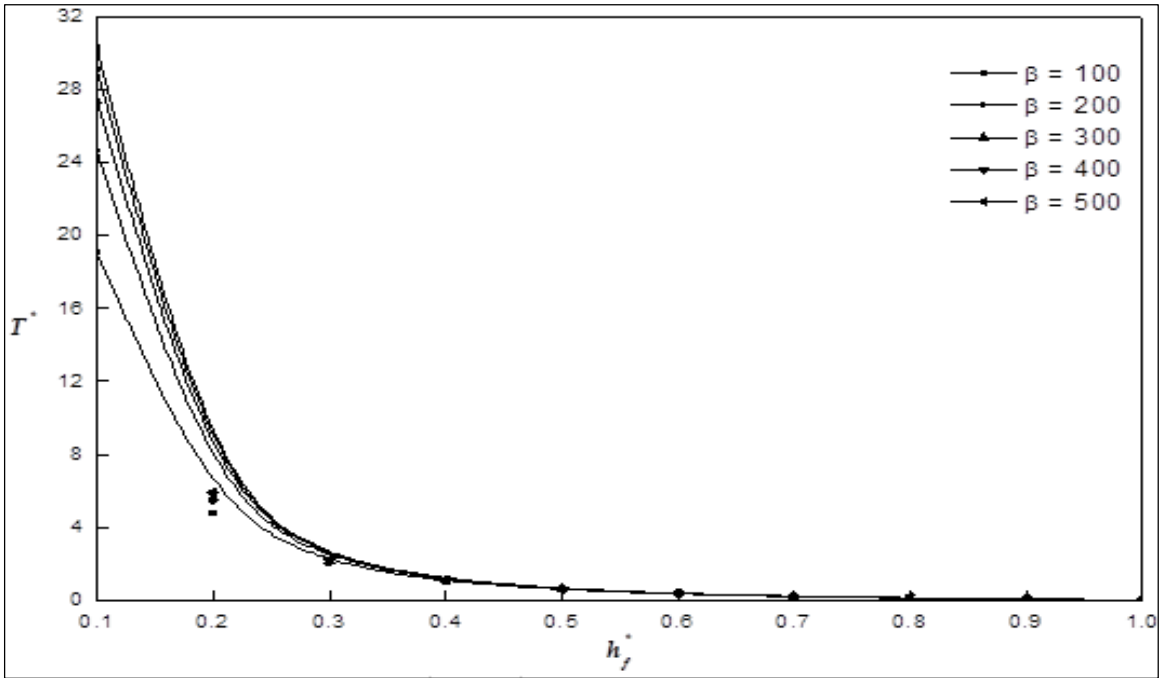

Fig 9: Variation of T^* with h_f^* for different values of β with $k = 3, a = 0.06$.

Figure 9, indicates variation of T^* with h_f^* for $\beta = 100$, $\beta = 200$, $\beta = 300$, $\beta = 400$ and $\beta = 500$. We observe that for any value of h_f^* dimensionless time T^* decreases for an increase in β.

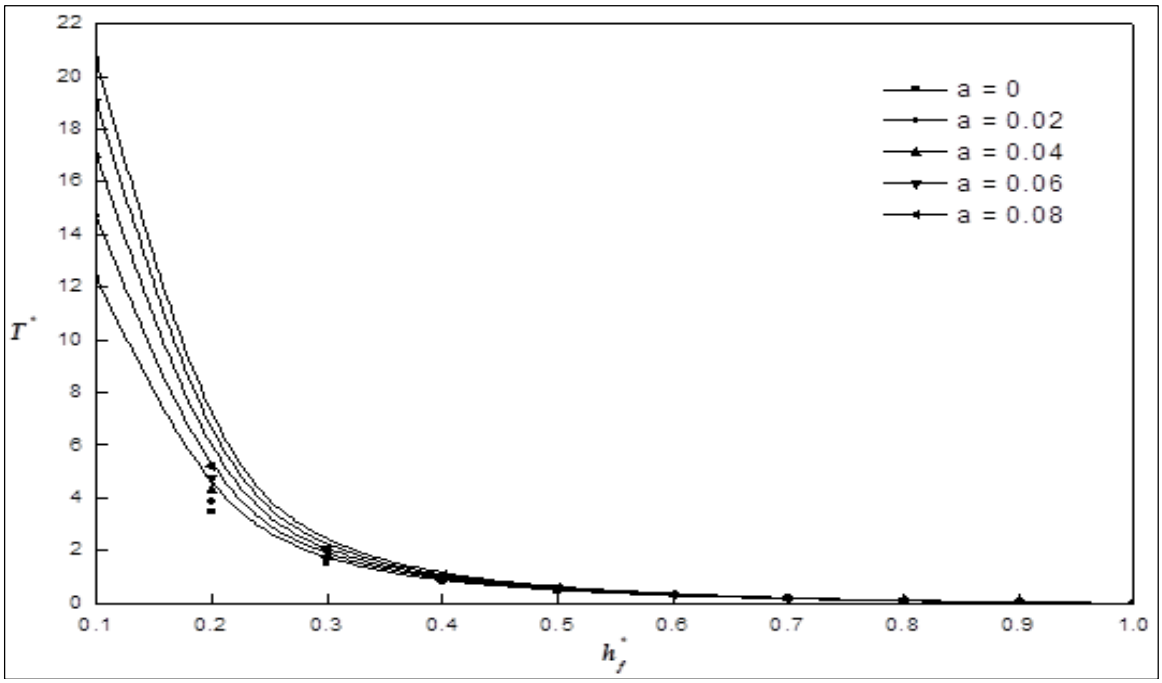

Fig 10: Variation of T^* with h_f^* for different values of a with $\beta = 100, k = 3$.

Figure 10, indicates variation of T^* with h_f^* for $a = 0$, $a = 0.02$, $a = 0.04$, $a = 0.06$ and $a = 0.08$. We observe that for any value of h_f^* dimensionless time T^* decreases for an increase in a.

5. Conclusion

The dimensionless pressure increases as the ratio of the viscosities increases. Also the dimensionless pressure increases when the slip parameter increases. The load carrying capacity increases as ratio of the viscosities increases. Also the load carrying capacity increases as the slip parameter increases. The load carrying capacity increases when the length of the triangle plate increases. The squeezing time decreases as ratio of the viscosities increases. Slip parameter increases as dimensionless squeeze time decreases.

Final film thickness increases as dimensionless squeeze time decreases. This indicates that when slip decreases the squeezing time also decreases.

6. References

1. Dowson D. A generalized Reynolds equation for fluid film lubrication. Inst. J Mech. Sic. 1962; 4:159-170.
2. Sudha V, Sundarammal kesavan, Ramamurhy V. Squeeze film characteristics of couple stress fluid between porous Triangular plates. Journal of Manufacturing Engineering, 2008, 3(1).
3. Vadher PA, Deheri G, Patel RM. Hydro magnetic Squeeze Film between Conducting Porous Transversely Rough Triangular Plates. J of Engg. Annals of Faculty of Engg. Hunedoara, 2008, 155-168.
4. Sundarammal kesavan, Manimegalai N. Surface Roughness Effect on the Squeeze Film between Two parallel Porous Elliptic Plates. Int. J Mathematical Modeling Simulation and Appilications. 2009; 2:427-39.
5. Patel RM, Deheri GM, Vadher PA. Performance of a Magnetic Fluid Based Squeeze Film between Transversely Rough Triangular Plates. Tribology in industry. 2010; 32:33-39.
6. Nitin Patel D, Gunamani Deheri. A Ferro fluid lubrication of a rough porous inclined slider bearing with slip velocity. Journal of Mech. Engg and Tech. 2012; 4(1):15-34.
7. Hamid khan, Islam S, Alishah JI. Comparison of different analytic solutions to axisymmetric squeezing fluid flow between two infinite parallel plates with slip boundary conditions. Hindawi, 2012, 1-18.
8. Sundarammal kesavan, Santhana Krishnan. Surface Roughness Effects on Squeeze film Behaviour in Porous Transversely Triangular Plates with Couple stress Fluid. International Journal of Numerical Methods for Heat & Fluid Flow. 2012; 3:1-12.
9. Rao RR, Gouthami K, Kumar JV. Effects of velocity-slip and viscosity variation in squeeze film lubrication of two circular plates. Tribology in Industry. 2013; 35:51-60.
10. Biradar Kashinath. Megneto hydrodynamic Couple stress Squeeze Film Lubrication of Triangular Plates. Int. J Engg. Inv. 2013; 3:66-73.
11. Fathima ST, Naduvinamani NB, Santhosh Kumar J. Megneto hydrodynamic Couple stress Squeeze Film Lubrication of Porous Plates. Indian J of Sci. and Tech. 2013; 6:209-214.
12. Khan U, Ahmed N, Khan SI, Ali Zaidi Z, Yang Xiao-Jun S, Din Tauseef Mohyud. On unsteady two-dimensional and axisymmetric squeezing flow between parallel plates. Alexandria Engg. Journal, 2014; 53:463-468.
13. Santhana Krishnan Narayanan, Sundarammal Kesavan. Magneto-Hydrodynamics non-newtonian squeeze film characteristics of porous curved circular plates. ARPN Journal of Engineering and Applied sciences. 2015; 10(14):5895-5907.
14. Thangavelu K, Sampathraj S, Sudha V. Effects of Viscosity Variation in squeeze film lubrication of circular stepped plates. International Journal of Mathematical Archive. 2018; 9(2):1-11.